JPE 9-2 -17

ICPE'07 Selected Paper

Feedback Linearization Control of Grid-Interactive PWM Converters with LCL Filters

Dong-Eok Kim* and Dong-Choon Lee†

†*Dept. of Electrical Eng., Yeungnam University, Gyeongsan, Korea

ABSTRACT

This paper proposes a feedback linearization control scheme of AC/DC PWM converters with LCL input filters using no damping resisters. Feedback linearization techniques use a transformation from nonlinear system models into equivalent linear models in a simpler form. The feedback linearization scheme in this work has cascade structures unlike usual feedback linearization, therefore it has an advantage that it is possible to limit the capacitor current to a certain level. The performance of the proposed controller is validated with simulation and experimental results.

Keywords: Feedback Linearization, PWM Converters, LCL Filters

1. Introduction

A three-phase AC/DC PWM converter with boost L filters has positive functions such as DC-link voltage control, sinusoidal input currents, unity power factor control, and bidirectional power flow. Furthermore, it is often utilized not only in a single AC/DC converter but also in back-to-back converters for AC machine drives and DFIG (Doubly-Fed Induction Generator) control for wind energy conversion systems as shown in Fig. 1 [1].

For wind-driven DFIG systems, since the output power is controlled through the back-to-back converters connected between the grid and the DFIG rotor side, improving converter control methods to cope with the grid disturbance and the quality of output power have been studied [2],[3]. However, it may also cause EMI problems to other sensitive equipment connected to the PCC (Point of Common Coupling) due to the switching-frequency related harmonic currents. Although this problem can be solved by increasing the boost inductor filter size, the cost of the inductor increases and the dynamic performance of the current control deteriorates.

To prevent these problems, LC or LCL filters can be used. With the LCL filters, the switching ripple components in grid currents are decreased with the same inductance value as that of LC-type filters while the dynamic performance is maintained [4]. Likewise, the low-pass filters of LCL type give significant advantages such as better capability of eliminating high frequency components and better harmonic performance at lower switching frequencies, etc. in higher-power applications [5]. However, for LCL filters, the resonance problem should be considered carefully. It is usually suppressed by the damping resisters connected in series with the filter capacitor. Although the resonance problem can be solved with the damping resistor, it is bulky and causes power

Manuscript received January 6, 2009; revised Feb. 23, 2009
†Corresponding Author: dclee@yu.ac.kr
Tel: +82-53-810-2582, Fax: +82-53-810-4767, Yeungnam Univ.
*Dept. of Electrical Eng., Yeungnam Univ., Gyeongsan, Korea

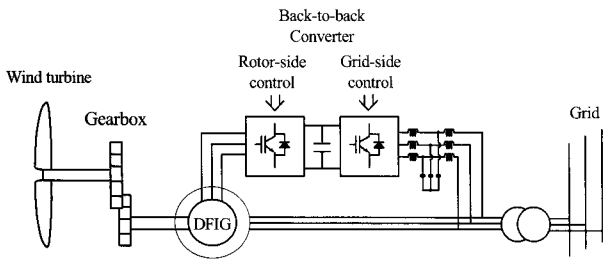

Fig. 1 DFIG wind turbine system

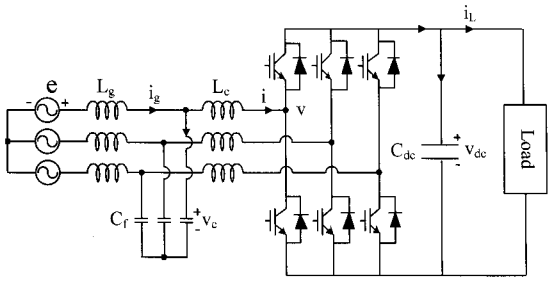

Fig. 2 AC/DC PWM converter with LCL filters

loss. Hence other attempts have been made such as active damping method [6] or virtual resister method [7]. However the active damping method needs the information of the filter parameters and the grid impedance. Also, the virtual resistor method needs the additional voltage sensors to measure the capacitor voltages. In [8], the active damping method applying a genetic algorithm was implemented without the parameter information and additional sensors. The multi-loop control method was investigated from the point of view that the capacitor is a source of resonance, where the capacitor current is measured and controlled as a minor control loop [9]. In [10], another method to solve the resonance problem by using a different combination of the measured variables from the sensors was proposed. In fact, if the converter input currents are measured and controlled, the system can be controlled stably with smaller damping resisters but it is difficult to obtain the unity power factor operation. Besides the above LCL filter-utilized applications, a resonant proportional control method with a compensator has been employed to reduce steady-state errors and achieve the improved startup operation [11]. In [12], a single-phase grid-interactive inverter topology has been proposed to prevent transient-state problems produced when entering an islanding fault mode in the distributed generation systems.

It is well known that the feedback linearization technique is a control method to eliminate the nonlinearity of the system by using inverse dynamics [13]. It has been applied to control the shunt active power filter [14] and the three-level NPC boost converter [15], which shows robust performance regarding disturbances as well as the fast transient responses.

In this paper, the feedback linearization is applied to control the AC/DC PWM converter with LCL input filters. At first, the converter system with LC filters is expressed in nonlinear equations. Then, they are linearized by applying the feedback linearization technique. For the linearized system, the tracking controller is designed by the linear control theory. Simulation results for the 2[MW] DFIG wind turbine system are illustrated and the experimental result verifies the effectiveness of the proposed control algorithm for the 3[kW] AC/DC PWM converter system.

2. AC/DC PWM Converters

2.1 Modeling of the system

Fig. 2 shows the AC/DC PWM converter with LCL input filters. L_g is grid-side inductance, L_c is converter-side inductance, C_f is filter capacitor. e is grid voltage, i_g is grid current, i is converter current, i_c is filter capacitor current, v_c is filter capacitor voltage. C_{dc} is DC-link capacitor, v_{dc} is DC-link voltage, and i_L is load current. The state equations of LCL filters and DC-link voltage are expressed in a d-q synchronous reference frame as in (1), which have converter input voltages as the inputs [16]. The DC-link voltage equation is obtained from the power balance between the AC input and the DC output of the PWM converters [17].

$$\begin{bmatrix} \dot{i}_{gd} \\ \dot{i}_{gq} \\ \dot{v}_{cd} \\ \dot{v}_{cq} \\ \dot{i}_d \\ \dot{i}_q \\ \dot{v}_{dc} \end{bmatrix} = \begin{bmatrix} 0 & \omega & -1/L_g & 0 & 0 & 0 & 0 \\ -\omega & 0 & 0 & -1/L_g & 0 & 0 & 0 \\ 1/C_f & 0 & 0 & \omega & -1/C_f & 0 & 0 \\ 0 & 1/C_f & -\omega & 0 & 0 & -1/C_f & 0 \\ 0 & 0 & 1/L_c & 0 & 0 & \omega & 0 \\ 0 & 0 & 0 & 1/L_c & -\omega & 0 & 0 \\ 0 & \dfrac{3e_q}{2C_{dc}v_{dc}} & 0 & 0 & 0 & 0 & 0 \end{bmatrix} \begin{bmatrix} i_{gd} \\ i_{gq} \\ v_{cd} \\ v_{cq} \\ i_d \\ i_q \\ v_{dc} \end{bmatrix} + \begin{bmatrix} 0 & 0 \\ 0 & 0 \\ 0 & 0 \\ 0 & 0 \\ -1/L_c & 0 \\ 0 & -1/L_c \\ 0 & 0 \end{bmatrix} \begin{bmatrix} v_d \\ v_q \end{bmatrix} + \begin{bmatrix} e_d/L_g \\ e_q/L_g \\ 0 \\ 0 \\ 0 \\ 0 \\ -i_L/C_{dc} \end{bmatrix} \tag{1}$$

where, e_d and e_q are d-q axis grid voltage, i_{gd} and i_{gq} are

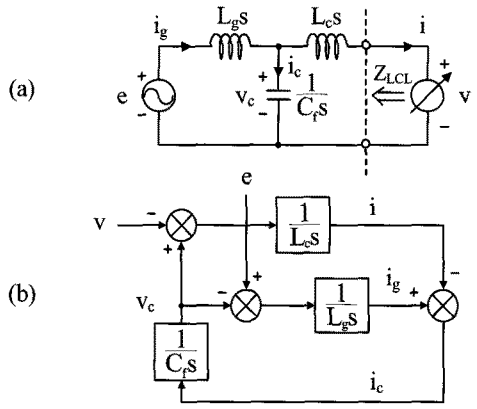

Fig. 3 Converter modeling (a) Per-phase equivalent circuit (b) Block diagram of transfer function

d-q axis grid currents, i_d and i_q are d-q axis converter currents, i_{cd} and i_{cq} are d-q axis filter capacitor currents, v_{cd} and v_{cq} are d-q axis filter capacitor voltages, and ω is grid angle frequency.

To control the PWM converter with LCL input filters without damping resisters which can stabilize the system from the resonance, the capacitor current regulation as an inner control loop is necessary [9]. Therefore, the state equations in (1) need to be modified into two state equations in order to realize the outer control loop and the inner control loop, where the former is needed in controlling both d-axis grid current for unity power factor and DC-link voltage, and the latter is needed for the capacitor current control. Two state equations are expressed as (2) and (3) which have the capacitor currents and the converter input voltages as the inputs, respectively.

$$\begin{bmatrix} \dot{i}_{gd} \\ \dot{i}_{gq} \\ \dot{v}_{cd} \\ \dot{v}_{cq} \\ \dot{v}_{dc} \end{bmatrix} = \begin{bmatrix} 0 & \omega & -\frac{1}{L_g} & 0 & 0 \\ -\omega & 0 & 0 & -\frac{1}{L_g} & 0 \\ 0 & 0 & 0 & \omega & 0 \\ 0 & 0 & -\omega & 0 & 0 \\ 0 & \frac{3e_q}{2C_{dc}v_{dc}} & 0 & 0 & 0 \end{bmatrix} \begin{bmatrix} i_{gd} \\ i_{gq} \\ v_{cd} \\ v_{cq} \\ v_{dc} \end{bmatrix} + \begin{bmatrix} \frac{1}{C_f} & 0 \\ 0 & \frac{1}{C_f} \\ 0 & 0 \\ 0 & 0 \\ 0 & 0 \end{bmatrix} \begin{bmatrix} i_{cd} \\ i_{cq} \end{bmatrix} + \begin{bmatrix} \frac{e_d}{L_g} \\ \frac{e_q}{L_g} \\ 0 \\ 0 \\ -\frac{i_L}{C_{dc}} \end{bmatrix} \quad (2)$$

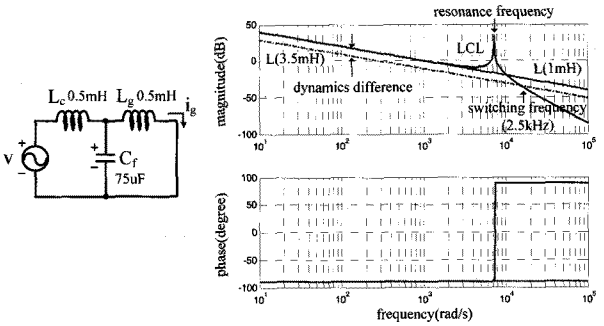

Fig. 4 Frequency response of LCL filters

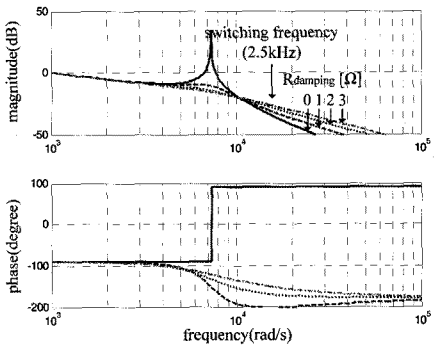

Fig. 5 Frequency response of LCL filters with damping resister

$$\begin{bmatrix} \dot{i}_{cd} \\ \dot{i}_{cq} \end{bmatrix} = \begin{bmatrix} 0 & \omega \\ -\omega & 0 \end{bmatrix} \begin{bmatrix} i_{cd} \\ i_{cq} \end{bmatrix} + \begin{bmatrix} \frac{1}{L_c} & 0 \\ 0 & \frac{1}{L_c} \end{bmatrix} \begin{bmatrix} v_d \\ v_q \end{bmatrix} + \begin{bmatrix} \frac{e_d - v_{cd}}{L_g} - \frac{v_{cd}}{L_c} \\ \frac{e_q - v_{cq}}{L_g} - \frac{v_{cq}}{L_c} \end{bmatrix} \quad (3)$$

Eqn. (2) shows non-linear state equations due to the non-linear DC-link voltage equation and (3) shows linear state equations. Appling the feedback linearization technique to both of the state equations, it is possible to control the outer loop for d-axis grid current control and DC-link voltage control and the inner loop of capacitor currents control.

2.2 LCL filters

The frequency responses of the L filters and the LCL filters are investigated to observe the attenuation of high frequency ripple components. Fig. 3(a) shows the per-phase equivalent circuit of the PWM converters in s-domain, and (b) shows the block diagram of the transfer function of the LCL filters. In Fig. 3(a), Thevenin equivalent impedance of the LCL filters is expressed as

$$Z_{LCL} = \frac{L_c L_g C_f s^3 + (L_c + L_g)s}{L_g C_f s^2 + 1} \quad (4)$$

The transfer function between the converter input voltage and the grid current is given from Fig. 3 (b) as

$$\frac{i_g(s)}{v(s)} = \frac{1}{L_c L_g C_f s^3 + (L_c + L_g)s} \quad (5)$$

Fig. 4 shows frequency responses of the L filter and LCL filters using (5). As shown in Fig. 4, the L filter and LCL filters with the same value of inductance have the same frequency responses in the low frequency region, but LCL filters are better in attenuating switching frequency-related harmonics. For the same performance, the inductance of L filter should be three times larger than that of the LCL-type, which results in degraded responses in the low frequency region. On the other hand, LCL-type filters could be unstable due to the resonance.

Fig. 5 shows a trade-off between the suppression of resonance and the elimination of switching frequency-related harmonics when damping resistor is used. It is noticed that the higher the value of damping resistor, the bigger the phase margin of LCL filters, but the performance decreases. Therefore, when using a damping resistor, an adequate trade-off should be met among the loss due to damping resistors, the system stability, and the performance of the filters.

Filter capacitors are a source of LCL resonance, which is known from (5). The resonance can be avoided by controlling capacitor currents directly.

3. Control of PWM Converters

The proposed control method with feedback linearization (henceforth 'FL') of PWM converter is composed of the outer control part for (2) and the inner control part for (3).

3.1 Outer control part

For applying the FL method, (2) is expressed as

$$\dot{x} = f(x) + gu \quad (6)$$

$$y = h(x) \quad (7)$$

where, $f(x) = \begin{bmatrix} f_1 \\ f_2 \\ f_3 \\ f_4 \\ f_5 \end{bmatrix} = \begin{bmatrix} e_d/L_g - \omega x_2 - x_3/L_g \\ e_q/L_g + \omega x_1 - x_4/L_g \\ +\omega x_4 \\ -\omega x_3 \\ \frac{3e_q x_2}{2C_{dc}x_5} - \frac{i_L}{C_{dc}} \end{bmatrix}$

$$x = \begin{bmatrix} x_1 & x_2 & x_3 & x_4 & x_5 \end{bmatrix}^T = \begin{bmatrix} i_{gd} & i_{gq} & v_{cd} & v_{cq} & v_{dc} \end{bmatrix}^T$$

$$g = \begin{bmatrix} 0 & g_2 & 0 & 0 & 0 \\ g_1 & 0 & 0 & 0 & 0 \end{bmatrix}^T = \begin{bmatrix} 0 & 1/C_f & 0 & 0 & 0 \\ 1/C_f & 0 & 0 & 0 & 0 \end{bmatrix}^T$$

The input variables are dq-axis capacitor currents and the output variables are d-axis grid current and DC-link voltage as,

$$u = \begin{bmatrix} u_1 & u_2 \end{bmatrix}^T = \begin{bmatrix} i_{cd} & i_{cq} \end{bmatrix}^T \quad | \quad y = \begin{bmatrix} y_1 & y_2 \end{bmatrix}^T = \begin{bmatrix} i_{gd} & v_{dc} \end{bmatrix}^T$$

Briefly, FL is to transform a non-linear plant to a linear plant consisting of simple integrators with feedback compensation, and it is started with making a direct relationship between input and output [18]. Accordingly, differentiation for the output is performed until the input appears, then (8) is obtained as

$$\begin{bmatrix} \ddot{y}_1 \\ \dddot{y}_2 \end{bmatrix} = A(x) + E(x) \begin{bmatrix} u_1 \\ u_2 \end{bmatrix} \quad (8)$$

where A(x) is an appendix matrix and E(x) is a decoupling matrix, which are expressed as

$$A(x) = \begin{bmatrix} A_1(x) & A_2(x) \end{bmatrix}^T \quad (9)$$

$$E(x) = \begin{bmatrix} -\frac{1}{L_g C_f} & 0 \\ 0 & \frac{3e_q}{2L_g C_f C_{dc} x_5} \end{bmatrix} \quad (10)$$

where,

$$A_1(x) = \omega f_2 - \omega \frac{x_4}{L_g}$$

$$A_2(x)=-\frac{3e_q f_2 f_5}{C_{dc}x_5^2}-\frac{3e_q x_2 \dot{f}_5}{2C_{dc}x_5^2}+\frac{3e_q x_2 f_5^2}{2C_{dc}x_5^3}-\frac{3e_q \omega f_1}{2C_{dc}x_5}+\frac{3\omega e_q x_3}{2L_g C_{dc}x_5}-\frac{\dot{i}_L}{C_{dc}}$$

$$\dot{f}_5=\frac{3e_q f_2}{2C_{dc}x_5}-\frac{3e_q x_2 f_5}{2C_{dc}x_5^2}-\frac{i_L}{C_{dc}}$$

The inputs to the nonlinear plant, which make it linearized by the compensation of the appendix matrix and the inverse matrix of the decoupling matrix, are given as

$$\begin{bmatrix}u_1\\u_2\end{bmatrix}=E^{-1}(x)\left[-A(x)+\begin{bmatrix}v_1\\v_2\end{bmatrix}\right] \tag{11}$$

where, $E^{-1}(x)=\begin{bmatrix}\hat{E}_{11}(x) & \hat{E}_{12}(x)\\ \hat{E}_{21}(x) & \hat{E}_{22}(x)\end{bmatrix}=\begin{bmatrix}-L_g C_f & 0\\ 0 & -\dfrac{2L_g C_f C_{dc}x_5}{3e_q}\end{bmatrix}$

v_1 and v_2 are the outputs of linear controllers. If (11) is substituted into (8), then the linear systems are obtained as

$$[\ddot{y}_1 \quad \ddot{y}_2]^{\mathrm{T}}=[v_1 \quad v_2]^{\mathrm{T}} \tag{12}$$

3.2 Inner control part

As explained in paragraph A, FL can be applied to linear state equations, so that linear plants are converted to simple integrators.

$$\dot{x}_{in}=f_{in}(x)+g_{in}u_{in} \tag{13}$$

$$y_{in}=h_{in}(x) \tag{14}$$

where, $f_{in}(x)=\begin{bmatrix}f_{in1}\\f_{in2}\end{bmatrix}=\begin{bmatrix}\omega x_{in1}+\dfrac{e_d-v_{cd}}{L_g}-\dfrac{v_{cd}}{L_c}\\ -\omega x_{in2}+\dfrac{e_q-v_{cq}}{L_g}-\dfrac{v_{cq}}{L_c}\end{bmatrix}$

$$x_{in}=[x_{in1} \quad x_{in2}]^{\mathrm{T}}=[i_{cd} \quad i_{cq}]^{\mathrm{T}}$$

$$g_{in}=\begin{bmatrix}g_{in1} & 0\\ 0 & g_{in2}\end{bmatrix}=\begin{bmatrix}1/L_c & 0\\ 0 & 1/L_c\end{bmatrix}$$

The input variables are d-q converter input voltages and the outputs variables are d-q capacitor currents as

$$u_{in}=[u_{in1} \quad u_{in2}]^{\mathrm{T}}=[v_d \quad v_q]^{\mathrm{T}} \mid y_{in}=[y_{in1} \quad y_{in2}]^{\mathrm{T}}=[i_{cd} \quad i_{cq}]^{\mathrm{T}}$$

Then, the inputs and outputs are related directly as

$$\begin{bmatrix}\dot{y}_{in1}\\ \dot{y}_{in2}\end{bmatrix}=A_{in}(x)+E_{in}\begin{bmatrix}u_{in1}\\u_{in2}\end{bmatrix} \tag{15}$$

The appendix and decoupling matrixes are given as

$$A_{in}(x)=\begin{bmatrix}A_{in1}(x)\\A_{in2}(x)\end{bmatrix}=\begin{bmatrix}\omega x_{in1}+\dfrac{e_d-v_{cd}}{L_g}-\dfrac{v_{cd}}{L_c}\\ -\omega x_{in2}+\dfrac{e_q-v_{cq}}{L_g}-\dfrac{v_{cq}}{L_c}\end{bmatrix} \mid E_{in}=\begin{bmatrix}1/L_c & 0\\ 0 & 1/L_c\end{bmatrix}$$

The inputs in the plant are expressed as (16)

$$\begin{bmatrix}u_{in1}\\u_{in2}\end{bmatrix}=E_{in}^{-1}\left[-A_{in}(x)+\begin{bmatrix}v_{in1}\\v_{in2}\end{bmatrix}\right] \tag{16}$$

where, $E_{in}^{-1}=\begin{bmatrix}L_c & 0\\ 0 & L_c\end{bmatrix}$

Applying FL to nonlinear plants, the decoupling matrix includes state variables. For linear plants, however, the elements of decoupling matrix consist of the constant.

3.3 Design of tracking controller

The controller used in the outer control loop is a linear tracking controllers, and the integrator controllers are added to reduce the steady state errors due to parameter variation and disturbance as [17], [19]

$$\begin{bmatrix}v_1\\v_2\end{bmatrix}=\begin{bmatrix}\ddot{y}_{1ref}-k_{11}\dot{e}_1-k_{12}e_1-k_{13}\int e_1\\ \ddot{y}_{2ref}-k_{21}\ddot{e}_2-k_{22}\dot{e}_2-k_{23}e_2-k_{24}\int e_2\end{bmatrix} \tag{17}$$

where, $e_1=y_1-y_{1ref}$, $e_2=y_2-y_{2ref}$, y_{ref} is tracking reference in which y_{1ref} is grid current reference and y_{2ref} is DC-link voltage reference. $k_{11,12,13}$ and $k_{21,22,23,24}$ are the gains of the controllers. The tracking control is completed with choosing gains by which the error dynamics converge to zero asymptotically. On the other hand, the controllers of the inner control loop do not include integrator controllers since the small steady state error of the inner control loop

does not affect the performance of the outer control loop. It is as

$$[v_{in1} \quad v_{in2}]^T = [-k_{in1}e_{in1} \quad -k_{in2}e_{in2}]^T \tag{18}$$

where, $e_{in1}=y_{in1}-y_{in1\text{-}ref}$, $e_{in2}=y_{in2}-y_{in2\text{-}ref}$, $y_{in1\text{-}ref}$ and $y_{in2\text{-}ref}$ means d and q-axis filter capacitor current references, respectively.

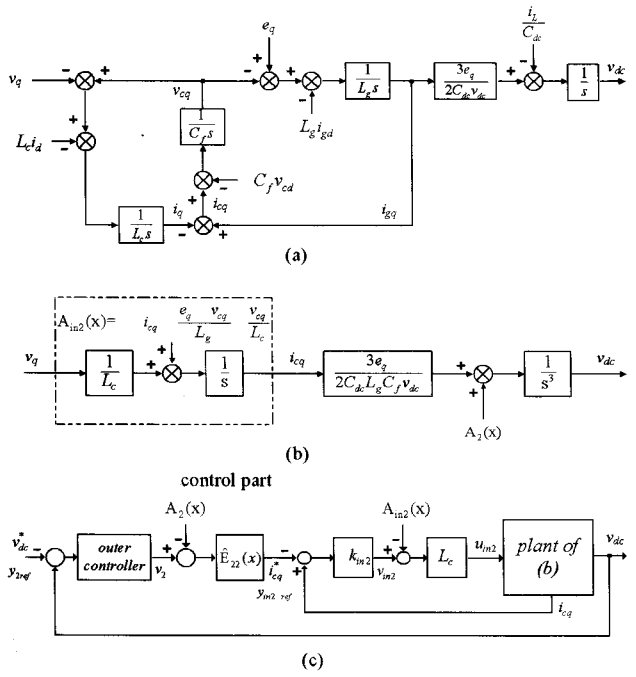

Fig. 6 Block diagrams of DC-link voltage plant
(a) Original (b) Rearranged
(c) Proposed FL method applied to (b)

Fig. 6 shows the block diagram for introducing the proposed FL method in controlling the DC-link voltage plant. Fig. 6(a) shows the original plant of DC-link voltage, and (b) shows the plant rearranged by (8), (15). In Fig. 6(c), the proposed FL method is applied to the plant of (b), where it is noticed that the plant can be analyzed as simple integrators if the matrixes are compensated from the control-part. Also, the inner control loop can be treated as a first order low-pass filter since the open-loop transfer function of the inner loop consists of the proportional gain and an integrator by the inverse-dynamics cancellation. Therefore, the output bandwidth of inner control loop can be properly limited by the proportional gain of the inner controller, where the proportional gain is identical to the bandwidth of the inner control loop. This means the resonance problem can be solved without a damping resister by choosing the bandwidth of the capacitor current control less than the resonance frequency of LCL filters. Additionally, the DC-link voltage, the control variable of the outer loop, is linearized by FL, so that it has better transient response. The reason is that the compensation of the appendix matrix A(x) and the inverse matrix of the decoupling matrix $E^{-1}(x)$ varying instantaneously with the state variables improve the transient response.

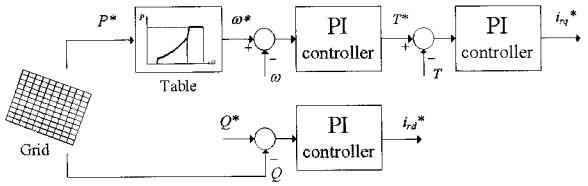

Fig. 7 MPPT control in DFIG wind turbine system

4. Simulation Results

In this simulation, a 2[MW] DFIG wind turbine system is applied. The rating of the PWM converter in the 2[MW] wind turbine system is about 30% of the wind turbine, which is 600[kW]. First, the simulation of the PWM converter itself is carried out, and then the PWM converter is embedded into the wind turbine system and simulated, which is controlled by MPPT (maximum power point tracking) control.

Fig. 7 shows the diagram of the MPPT control algorithm of DFIG [20], [21]. The P^* is power measured at the grid. The Q^* and Q are reactive power reference and reactive power measured at the grid, respectively. The ω^* and ω are DFIG speed reference and real speed. The T^* and T are torque reference and real torque value. The i_{rd}^* and i_{rq}^* are the d-and q-axis rotor current references. The DFIG is controlled based on the stator flux-oriented vector control technique. In Fig. 7, the ω^* is extracted from the pre-determined table for MPPT.

The performance comparison between the PI controllers and the proposed method ('FL') is carried out. In the PI control method, the grid voltages and currents are measured. The grid currents and DC-link voltage are

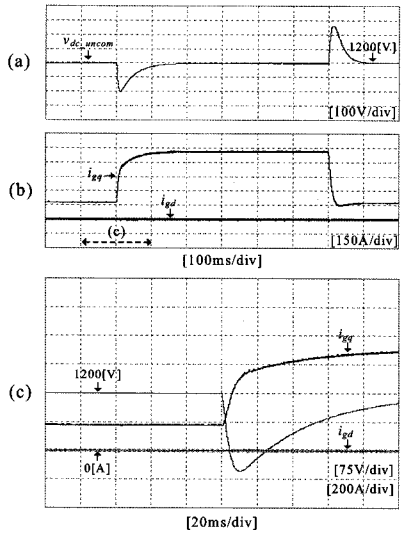

Fig. 8 PI control without load current compensation
(a) DC-link voltages
(b) Dq-axis grid currents
(c) Enlarged figure

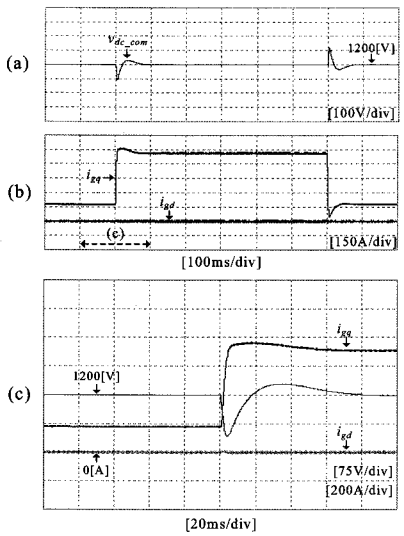

Fig. 9 PI control with load current compensation
(a)DC-link voltages
(b) Dq-axis grid currents
(c) Enlarged figure

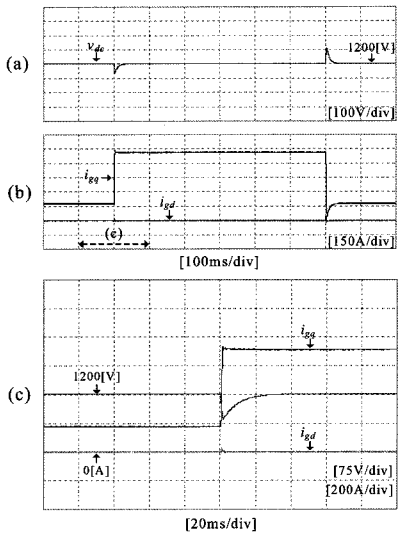

Fig. 10 Proposed control ('FL')
(a) DC-link voltage
(b) Dq-axis grid currents
(c) Enlarged figure

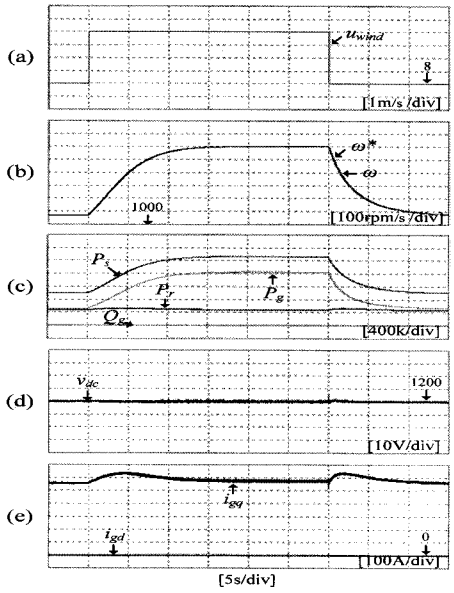

Fig. 11 FL in DFIG wind turbine system
(a) Wind speed
(b) DFIG speed
(c)Active (P_s: stator-side, P_r: rotor-side, P_g: grid-side) and reactive (Q_g: grid-side) power
(d) DC-link voltage
(e) Dq-axis grid currents

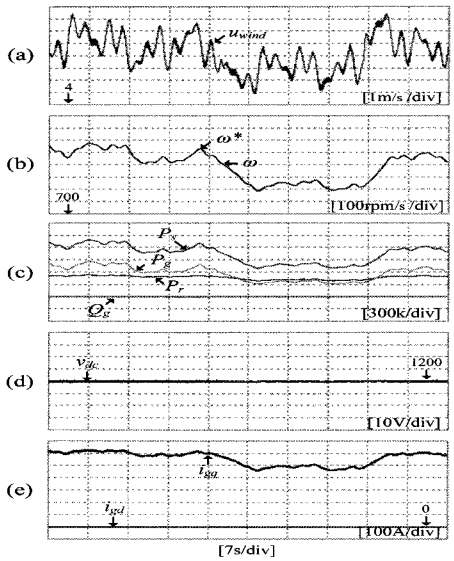

Fig. 12 FL in DFIG wind turbine system with real wind speed profile
(a) Wind speed
(b) DFIG speed
(c) Active (P_s: stator-side, P_r: rotor-side, P_g: grid-side) and reactive (Q_g: grid-side) power
(d) DC-link voltage
(e) Dq-axis grid currents

controlled with PI controllers, and DC-link voltage controller includes the feedforward compensation of load current. For FL, the grid voltages and currents, and capacitor currents are measured, and the capacitor voltage is estimated. In all cases, DC-link voltage is controlled at 1200[V] and d-axis grid current is controlled at zero for unity power factor. System parameters for the simulation are shown in Table 2 in Appendix.

Resistive loads of 9.6[Ω] are applied during the full period of simulation from the start. To observe the response performance in transient state, additional resistive loads of 3.2[Ω] are applied to the resistive loads of 9.6[Ω] in parallel and unloaded abruptly. Fig. 8 and 9 show the transient responses in case of PI controls with 1[Ω] damping resistors, which are with and without load current compensation, respectively. Fig. 10 shows the transient responses of FL which does not use damping resistors. The FL shows the better performance than PI and even PI with load compensation.

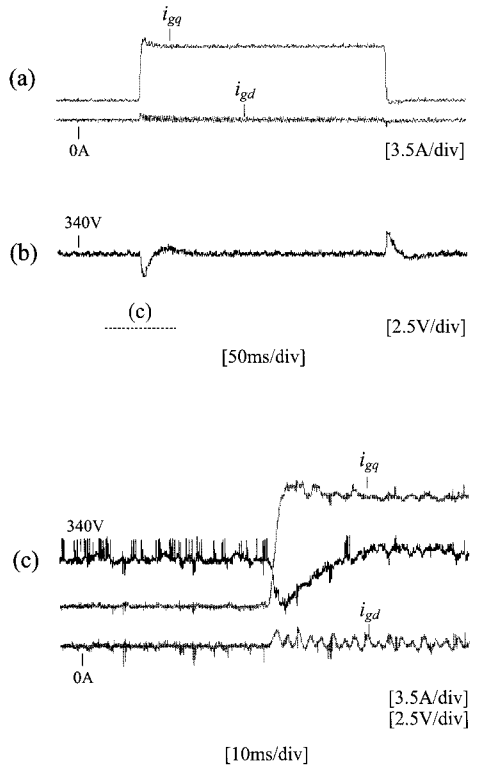

Fig. 13 PI controller with load current compensation
(a) Dq-axis currents (b) DC-link voltage
(c) Zoom in of (a) and (b)

Then, the FL is applied to the grid side converter in DFIG wind turbine system, which is shown in Fig. 1. The DFIG wind turbine is controlled with MPPT. The parameters for the wind turbine system are shown in Appendix.

Fig. 11 shows the performance of the FL when the wind speed changes in step from 8[m/s] to 12[m/s] and back to 8[m/s]. Fig. 11(a) shows the wind speed, (b) shows that the speed of DFIG which slowly changes due to high inertia and settles to the maximum power point, and (c) shows the active powers of the stator, rotor, grid and the reactive power of the grid. (d) and (e) show the DC-link voltage and dq-axis grid currents, respectively. Since the speed of DFIG varies slowly due to large moments of inertia, severe transient states do not occur.

Fig. 12 shows the same performance as in Fig. 11 for a real wind speed profile.

5. Experimental Results

To validate the proposed method, the experiment has been performed. The actual operation of the IGBT PWM converter was tested on a small prototype. The parameters for the PWM converter and gains of controllers are shown in Table 3 in the Appendix.

The gains of the PI controller are determined based on the P gain of the proposed FL method. The P gain of PI controllers is set at double the production of k_{23} and $(2 \cdot L_g \cdot C_f \cdot C_{dc} \cdot v_{dc}/(3 \cdot e_q))$ where v_{dc} is 340[V], and e_q is 180[V].

To observe the transient performance, 750[W] loads are applied during the entire experiment, then an additional 2.25[kW] load is applied abruptly for 300[ms]. Because the source voltage at the laboratory is distorted, the 5^{th} and 7^{th} harmonic current controllers are added to the basic current controller for both the PI and FL control methods. Fig. 13 shows the performance of PI controllers in transient state. The DC-link voltage is disturbed about 2.7[V] and overshoots are observed. Fig. 14 shows the performance of the proposed method. The DC-link voltage is varied about 1.5[V] and recovered rapidly to the reference value without overshoot.

To observe the tracking performance, the reference of the DC-link voltage is changed in step from 320[V] to 360[V].

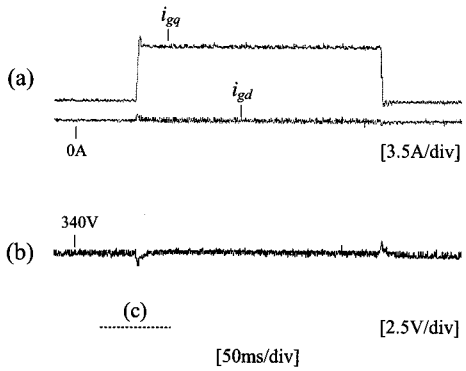

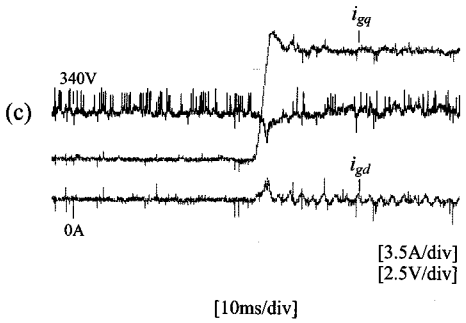

Fig. 14 FL (a) Dq-axis currents (b) DC-link voltage (c) Zoom in of (a) and (b)

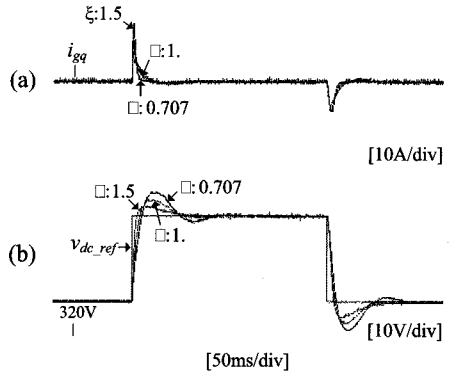

Fig. 15 Tracking performance of PI controller

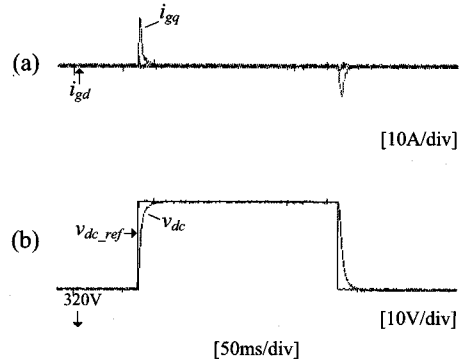

Fig. 16 Tracking performance of FL

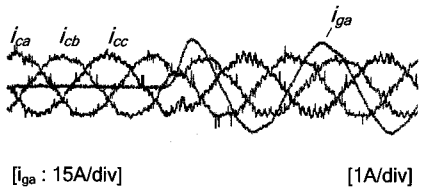

Fig. 17 Capacitor and grid current waveforms

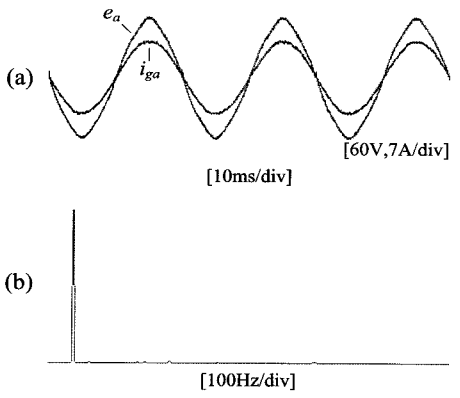

Fig. 18 Waveforms and FFT analysis (a) Grid voltage and grid current (b) Harmonic spectrum of grid current

Fig. 15 and 16 show the tracking performance of PI and the proposed methods, respectively. In PI control, ξ is varied from 0.707 to 1.5. It is observed that overshoots still exist in Fig. 15. On the other hand, the proposed method shows good performances without overshoot and steady state error as shown in Fig. 16.

Fig. 17 shows the variation of the capacitor and grid currents when the load is changed. The amplitude of capacitor currents is little changed, but the phases of capacitor currents are jumped and the grid currents are increased.

Fig. 18 shows the waveforms of the grid voltage and current, and harmonic spectrum of the grid current when FL is applied. The grid voltage is distorted, but the grid current is controlled in sinusoid.

Table 1 lists the harmonic analysis of PI and FL methods. Both of them show good results less than 1.4[%]. However, FL gives better performance in attenuating the switching ripples since damping resisters are not used.

6. Conclusions

In this paper, the feedback linearization for the control of the three-phase PWM converter with LCL input filters has been proposed. The size of filter inductors in the case of the LCL filters can be made smaller than the L filter for the same filtering effect of the switching frequency-related harmonic components. Better performance in suppression of switching ripples compared to the L filter was obtained, and the resonance problem of the LCL filters was solved without using damping resisters. Filter capacitor currents have been controlled with a proportional tracking controller; therefore the resonance problem of LCL filters has been successfully solved. Furthermore, DC-link voltage control performance in transient state has been enhanced by cancelling nonlinearity of the DC-link voltage plant owing to the utilized feedback linearization method. The enhanced performance is confirmed by comparing the proposed method with the PI controller.

Acknowledgement

This work has been supported by KESRI (R-2005-7-067), which is funded by MKE (Ministry of Knowledge Economy).

Appendix

Table 1 Analysis of THD

Controller type	THD	Switching ripple
PI controller with compensation	1.34 %	1.0 %
Feedback linearization method	1.25 %	0.3 %

Table 2 System parameters for simulation

	Parameters
AC-DC PWM converter with LCL filters (Fig. 2)	e_{line} (grid line-voltage): 690Vrms C_{dc} (DC-link capacitor): 8000[uF] f_{sw} (switching frequency): 2.5[kHz] f_s (sampling frequency): 5[kHz] L_g: 0.5[mH], L_c: 0.5[mH], C_f: 75[uF] $R_{damping}$(damping resister for PI control): 1[Ω] $f_{LCL\text{-}res}$ (resonance frequency) : 1.16[kHz]
Wind turbine (Fig. 1)	Blade diameter: 80[m] Gear ratio: 1:80 Total moment of inertia: $3.1\cdot10^6$ [kg.m^2]
DFIG (Fig. 1)	Power rating: 2[MW] Voltage rating: 690[V] Base frequency: 60[Hz] Number of poles: 4 Magnetizing inductance: 3.95279[p.u] Stator resistance: 0.00488[p.u] Stator leakage inductance: 0.09241[p.u] Rotor resistance: 0.00549[p.u] Rotor leakage inductance: 0.09955[p.u]

Table 3 System and controller parameters for experiments

		Parameters
AC/DC PWM converter with LCL filters		e_{line}: 220Vrms C_{dc}: 1950[uF] f_{sw}: 5[kHz], f_s: 10[kHz] L_g: 0.8[mH], L_c: 2[mH], C_f: 10[uF] $R_{damping}$(for PI control): 5[Ω] $f_{LCL\text{-}res}$: 2.1[kHz]
Gains of controllers	PI	▪ DC-link voltage controller (outer loop) P controller: $2\cdot\xi\cdot\omega_{dc}\cdot C_{dc} = 0.25$ I controller: $\omega_c^2\cdot C_{dc} = 15.8$ ($\xi = 0.707$, $\omega_{dc} = 90$) ▪ Grid current controller (inner loop) P controller: $\omega_{cur}\cdot(L_g+L_c) = 14.0$ I controller: $\omega_{cur}\cdot 0.01 = 50.0$ ($\omega_{cur} = 5000$)
	FL	▪ Outer loop tracking controller k_{11}: 1.35×10^4 k_{21}: 1×10^4 k_{12}: 2.7×10^7 k_{22}: 3.15×10^7 k_{13}: 2.7×10^8 k_{23}: 6×10^9 k_{24}: 6×10^{10} ▪ Inner loop tracking controller k_{in1}: 8×10^3 k_{in2}: 8×10^3

References

[1] J. Yao, H. Li, Y. Liao, and Z. Chen, "An improved control strategy of limiting the DC-link voltage fluctuation for a doubly fed Induction wind generator", *IEEE Trans. Power Electron.*, Vol. 23, No. 3, pp.1205-1213, May 2008.

[2] O. S. Ebrahim, P. K. Jain, and G. Nishith, "New control scheme for the wind-driven doubly fed induction generator under normal and abnormal grid voltage conditions",

Journal of Power Electronics, Vol. 8, No. 1, pp. 10-22, Jan. 2008.

[3] G.-B. Chung and J. Choi, "Application of fuzzy PI control algorithm as stator power controller of a doubly-fed induction machine in wind power generation systems", *Journal of Power Electronics*, Vol. 9, No. 1, pp. 109-116, Jan. 2009.

[4] J.-S. Noh, J. Choi, "Design of Voltage Source PWM Converter with AC Input LCL Filter", *KIPE Trans.*, Vol. 3, pp. 490-498, 2002.

[5] G. Shen, D. Xu, L. Cao , and X. Zhu, "An improved control strategy for grid-connected voltage source inverters with an LCL filter", *IEEE Trans. Power Electron.*, Vol. 23, No. 4, pp.1899-1906, July 2008.

[6] M. Liserre, A. Dell'Aquila, and F. Blaabjerg, "Stability improvements of an LCL-filter based three-phase active rectifier", *IEEE PESC. Proc.*, Vol. 3, pp. 1195-1201, June 2002.

[7] P. A. Dahono, Y. R. Bahar, Y. Sato, and T. Kataoka, "Damping of transient oscillations on the output LC filter of PWM inverters by using a virtual resistor", *IEEE PEDS. Proc.*, Vol. 1, pp.403-407, Oct. 2001.

[8] M. Liserre, A. Dell'Aquila, and F. Blaabjerg, "Genetic Algorithm-Based Design of the Active Damping for an LCL-Filter Three-Phase Active Rectifier", *IEEE Trans. Power Electron.*, Vol. 19, No. 1, pp.76-86, Jan. 2004.

[9] T. Erika, and D. G. Holmes, "Grid current regulation of a three-phase voltage source inverter with an LCL input filter", *IEEE Trans. Power Electron.*, Vol. 18, No. 3, pp. 888-895, May 2003.

[10] R. Teodorescu, F. Blaabjerg, M. Liserre, and A. Dell'Aquila, "A stable three-phase LCL-filter based active rectifier without damping", *IEEE IAS Proc.*, Vol. 3, pp. 1552-1557, Oct. 2003.

[11] S.-Y. Park, and C.-L. Chen, J.-S. Lai, and S.-R. Moon, "Admittance compensation in current loop control for a grid-tie LCL fuel cell inverter", *IEEE Trans. Power Electron.*, Vol. 23, No. 4, pp.1716-1723, July 2008.

[12] H. Kim, T. Yu, and S. Choi, "Indirect current control algorithm for utility interactive inverters in distributed generation system", *IEEE Trans. Power Electron.*, Vol. 23, No. 3, pp.1342-1351, May 2008.

[13] T.-S. Lee, "Input-output linearization and zero-dynamics control of three-phase AC/DC voltage-source converters", *IEEE Trans. Power Electron.*, Vol. 18, No. 10, pp.1625-1631, Jan. 2003.

[14] N. Mendalek, K. Al-Haddad, F. Fnaiech, and L. A. Dessaint, "Nonlinear control technique to enhance dynamic performance of a shunt active power filter", *IEE Proc. Elect. Power Applicat.*, Vol. 150, pp. 373-379, July 2003.

[15] L. Yacoubi, K. Al-Haddad, L.-A. Dessaint, and F. Fnaiech, "Linear and nonlinear control techniques for a three-phase three-level NPC boost rectifier", *IEEE Trans. Ind. Electron.*, Vol. 53, No. 6, pp.1908-1918, Dec. 2006.

[16] M. Liserre, A. Dell'Aquila, and F. Blaabjerg, "An overview of three-phase voltage source active rectifier interfacing the utility," *IEEE Power Tech. Conf. Proc.*, Vol. 3, June 2003.

[17] D.-C. Lee, G.-M. Lee, and K.-D. Lee, "DC-bus voltage control of three-phase AC/DC PWM converters using feedback linearization", *IEEE Trans. Ind. Applicat.*, Vol. 36, No. 3, pp. 826-833, May-June 2000.

[18] J. E. Slotine and W. Li, "Applied Nonlinear Control", Prentice Hall, pp.207-271, 1991.

[19] M. M. Seron, S. F. Graebe, and G. C. Goodwin, "All stabilizing controllers, feedback linearization and anti-windup: a unified review", *American Control Conf.*, Vol. 2, pp.1685-1689, July 1994.

[20] A. G. Abo-Khalil and D.-C. Lee, "MPPT control of wind generation systems based on estimated wind speed using SVR", *IEEE Trans. Ind. Electron.*, Vol.55, No.3, pp. 1489-1490, Mar. 2008.

[21] K. Protsenko and D. Xu, "Modeling and control of brushless doubly-fed induction generators in wind energy applications", *IEEE Trans. Power Electron.*, Vol.23, No.3, pp.1191-1197, May 2008.

[22] M. Liserre, A. Dell'Aquila, and F. Blaabjerg, "An overview of three-phase voltage source active rectifier interfacing the utility", *IEEE Power Tech. Conf. Proc.*, vol. 3, June 2003.

[23] D.-C. Lee, G.-M. Lee, and K.-D. Lee, "DC-bus voltage control of three-phase AC/DC PWM converters using feedback linearization", *IEEE Trans. Ind. Applicat.*, Vol. 36, No. 3, pp. 826-833, May-June 2000.

[24] J. E. Slotine and W. Li, "Applied Nonlinear Control", Prentice Hall, pp.207-271, 1991.

[25] M. M. Seron, S. F. Graebe, and G. C. Goodwin, "All stabilizing controllers, feedback linearization and anti-windup: a unified review", *American Control Conf.*, Vol. 2, July 1994, pp.1685-1689.

[26] A. G. Abo-Khalil and D.-C. Lee, "MPPT control of wind generation systems based on estimated wind speed using SVR", *IEEE Trans. Ind. Electron.*, Vol. 55, No. 3, pp. 1489-1490, Mar. 2008.

[27] K. Protsenko and D. Xu, "Modeling and control of brushless doubly-fed induction generators in wind energy applications", *IEEE Trans. Power Electron.*, Vol. 23, No.3, pp.1191-1197, May 2008.

Dong-Eok Kim received the B.S. and M.S. in electrical engineering from Yeungnam University, Gyeongsan, Korea, in 2005 and 2008, respectively. He was an engineer with LG Philips LCD (LG Display) at 2005. Since 2008, he has been a research engineer in the Electrical Technology Research Department, Institute of Information and Communication, Yeungnam University. His research interests are power converter control, motor control, power quality, and fault diagnosis.

Dong-Choon Lee received the B.S., M.S., and Ph.D. degrees in electrical engineering from Seoul National University, Seoul, Korea, in 1985, 1987, and 1993, respectively. He was a Research Engineer with Daewoo Heavy Industry from 1987 to 1988. Since 1994, he has been a faculty member of the Dept. of Electrical Engineering, Yeungnam University, Gyeongbuk, Korea. As a Visiting Scholar, he joined Power Quality Laboratory, Texas A&M University, College Station in 1998, and Electrical Drive Center, University of Nottingham, U.K. in 2001, and Wisconsin Electric Machines & Power Electronic Consortium, University of Wisconsin, Madison in 2004. His research interests include ac machine drives, control of power converters, wind power generation, and power quality. Dr. Lee is currently a Publication Editor of Journal of Power Electronics, the Korean Institute of Power Electronics.